https://doi.org/10.5194/egusphere-2026-4390
Preprint. Discussion started: 4 August 2026

Observed Yanai wave trajectories in the Western Equatorial Atlantic

Alexandra Andrae[1], Peter Brandt[1,2], Franz Philip Tuchen[3], Rebecca Hummels[1], and Joke F. Lübbecke[4,5]

[1]GEOMAR Helmholtz Centre for Ocean Research Kiel, Kiel, Germany
[2]Faculty of Mathematics and Natural Sciences, Kiel University, Kiel, Germany
[3]Rosenstiel School of Marine, Atmospheric, and Earth Science, University of Miami
[4]Institute of Environmental Physics, University of Bremen, Bremen, Germany
[5]MARUM – Center for Marine Environmental Sciences, University of Bremen, Bremen, Germany

Correspondence: Alexandra Andrae (aandrae@geomar.de)

Abstract. The western equatorial Atlantic Ocean features a variety of dynamical processes. The upper-ocean circulation is characterized by both western boundary currents and the equatorial current system, which are important pathways of the upper branch of the Atlantic Meridional Overturning Circulation. On subseasonal to seasonal timescales, equatorial waves such as Yanai waves further influence local ocean dynamics. Yanai waves, also referred to as mixed Rossby-gravity waves, exist in all tropical ocean basins predominantly on timescales of 10 to 30 days. They are associated with meridional velocities at the equator, setting them apart from other equatorial waves. While Yanai waves have been thoroughly analyzed regarding their energy dissipation, generation mechanisms, and propagation characteristics, little observational evidence has been provided regarding their surface trajectories. This study investigates the trajectories of Lagrangian surface drifters with respect to the presence of Yanai waves in the western equatorial Atlantic. Only few surface drifters remain long enough at or close to the equator to offer insights into equatorial phenomena since the prevailing poleward Ekman flow near the equator typically drives drifters to higher latitudes fairly quickly, which makes measurements sparse but particularly valuable. During a research cruise in May 2023, eight surface drifters were deployed into the western boundary current system off Brazil along 35 °W between the equator and 2.25 °S. Three of these drifters got trapped within circling surface movements centered around the equator. Our analysis suggests that this circular movement can be attributed to a Yanai wave. First, we find that the drifter oscillations coincided with cross-equatorial fluctuations of the meridional velocity component of the wind, a commonly accepted generation mechanism of Yanai waves. Additionally, we could reproduce the observed trajectories by conducting a series of numerical experiments with artificial drifters, combining the mean background flow of the area with theoretical Yanai wave-induced surface velocities. The observed Yanai wave is characterized by a 14-day period and velocity amplitudes of approximately 0.6 to 0.7 $\mathrm{m\,s^{-1}}$.

1 Introduction

Yanai waves are equatorial waves that are observed in all ocean basins. They influence various tropical oceanic and atmospheric phenomena and dynamics such as the Indian monsoon (e.g. Luyten and Roemmich, 1982; Schott and McCreary, 2001;

https://doi.org/10.5194/egusphere-2026-4390
Preprint. Discussion started: 4 August 2026

Chatterjee et al., 2013), the Madden-Julian-Oscillation (Takasuka and Satoh, 2020), or the heat and momentum budget in the tropics (e.g. Weisberg et al., 1979). Yanai waves exhibit an eastward group velocity across all wavenumbers, transporting energy eastward and, if generated at the surface, downward. At large negative wavenumbers, Yanai waves exhibit westward phase propagation, while at large positive wavenumbers, they resemble eastward-propagating Kelvin waves. Therefore, they are also often referred to as mixed Rossby-gravity waves. Observational evidence of Yanai waves in the atmosphere was provided almost contemporaneously with their theoretical formulation (mathematical solution: Yanai and Maruyama (1966); Matsuno (1966); observation: Yanai and Hayashi (1969)). In the ocean, Yanai waves were first observed through the analysis of sea level records from Pacific islands (Wunsch and Gill, 1976). Now, observational data from ocean current meters monitoring the vertical water column (Zhu et al., 1998; David et al., 2011; Farrar and Durland, 2012; Nagura and McPhaden, 2023, 2024; Terada and Masumoto, 2025; Zhang et al., 2025), moored measurements at the equator (Tuchen et al., 2018), Argo data (Terada and Masumoto, 2025), or satellite altimetry and satellite-derived sea surface temperatures (Wakata, 2007; Shinoda, 2012) are used to describe these waves. Furthermore, ocean models have been utilized to explain both deep and upper ocean intraseasonal velocity variability (Sengupta et al., 2001; Körner et al., 2022), or to quantify their spatial and temporal structures (e.g. Chatterjee et al., 2013).

While Yanai waves in the atmosphere are observed at periods of 2 to 6 days (e.g. Wheeler et al., 2000; Magaña and Yanai, 1995; Braga and Magaña, 2025), observations in the ocean show longer periods from 10 to 30 days (Shinoda, 2012). More precisely, there are two peaks in the energy spectrum at biweekly (10-20 days) and monthly (20-30 days) periods. Biweekly Yanai waves are often observed close to the surface and are generated by cross-equatorial wind stress (McPhaden and Picaut, 1990; Zhu et al., 1998; Zhang et al., 2025; Wang et al., 2026), whereas monthly Yanai waves, which are found at intermediate depths, are more often attributed to barotropic shear instabilities between zonal equatorial currents (e.g. von Schuckmann et al., 2008; Körner et al., 2022; Nagura and McPhaden, 2023, 2024; Zhang et al., 2025; Terada and Masumoto, 2025; Wang et al., 2026).

Yanai waves have been frequently observed in the Pacific and Indian oceans, but less so in the western tropical Atlantic even though they are known to play a role in shaping intraseasonal variability in the tropical Atlantic (e.g. Weisberg and Horigan, 1981; Shinoda, 2012).

In the western tropical Atlantic, the upper-ocean mean state circulation is characterized by both western boundary currents and the equatorial current system. Furthermore, the flow of subtropical cells contributes to the surface circulation and thermocline. Subtropical cells are shallow meridional overturning cells that connect the upwelling regions at the equator and in the eastern part of the ocean basin with the downwelling that occurs within the subtropical gyres (Tuchen et al., 2020). The currents at the western boundary also contribute to the Atlantic Meridional Overturning Circulation (Tuchen et al., 2022b).

Additionally, the easterly trade winds directly drive westward surface currents known as the northern and branches of the central South Equatorial Current. These westward currents cause warm and salty water to accumulate in the western tropical Atlantic. Consequently, the mixed layer deepens in the west. At the western boundary, the North Brazil Current (NBC) accomplishes the upper ocean cross-equatorial transport. At about 3-8 °N, the NBC separates from the coast, meanders, and

https://doi.org/10.5194/egusphere-2026-4390
Preprint. Discussion started: 4 August 2026

partly retroflects southeastward into the North Equatorial Countercurrent. Here, eddies called the NBC rings are generated, propagating northwestward (e.g. Schott et al., 1998; Jochum and Malanotte-Rizzoli, 2003; Aguedjou et al., 2019).

Thus, circling motions in the region from 3-8 °N are mostly associated with NBC rings, however, we observed circling motions of a different origin. Past studies give little evidence concerning the surface trajectories of Yanai waves and how they can be observed. This study investigates the trajectories of Lagrangian surface drifters regarding the possibility that the presence of Yanai waves could influence their movement. Only few surface drifters stay long enough at or close to the equator to give insights about these equatorial phenomena. The equatorial upwelling caused by poleward Ekman flow usually drives drifters to higher latitudes fairly fast. In June 2023, three drifters stayed long enough at the equator to observe a circling motion. During the research cruise MSM117 eight drifters were deployed along 35 °W close to the equator. Three drifters deployed south of the equator departed northward with the strong coastal NBC to reach the equator, where they completed circles with exactly the same period despite having different radii (Fig. 2). In this study, we investigate the cause of this circular motion and suggest that it can be partly attributed to a Yanai wave with a 14-day period.

This study is structured as follows: Section 2 gives a short overview of the data and methods that are used in this study. Second, the observed situation by the ocean drifters is briefly described, and biweekly fluctuations of meridional wind and surface currents are analyzed regarding the signal of a 14-day Yanai wave. Third, the results of numerical experiments with the artificial drifters that reconstruct the observations are discussed. The last section gives a short summary and future outlook.

2 Data and Methods

2.1 Data

The wind data used is the Cross-Calibrated Multi-Platform (CCMP) wind vector analysis product version-3.1 (Mears et al., 2022). CCMP Version-3.1 vector wind analyzes are produced by Remote Sensing Systems. Data are available at www.remss.com, last access: 30 June 2026. This study has been conducted using E.U. Copernicus Marine Service Information; DOI (product): https://doi.org/10.48670/moi-00021,https://doi.org/10.3389/feart.2021.698876, last access: 30 June 2026. The gridded Level 4 data is a combination of the (adjusted) ERA5 reanalysis as background field and a wide range of observational satellite data, including the scatterometers QuikScat, ASCAT-A and ASCAT-B, as well as the SSM/I, SSMIS, TMI, GMI, ASMR-E, AMSR2, and WindSat radiometers. The data have been validated using in situ buoy- and airborne measurements as well as saildrones and oil platforms. The data are delivered at a temporal and spatial resolution of six hours and 0.25 °, respectively, and represent winds at 10 m above the sea surface. For this work, daily averages were used. The wind speed is given in meters per second.

The ocean current data are taken from the global ocean physics reanalysis 'GLORYS12V1' product by the Copernicus Marine Service (CMEMS, Jean-Michel et al. (2021)). It is eddy-resolving with a 1/12 ° horizontal resolution with 50 vertical levels. The level 4 data is based on the Nucleus for European Modelling of the Ocean (NEMO) platform with the European Centre for Medium-Range Weather Forecasts' (ECMWF) ERA-Interim and ERA5 reanalyses as surface forcing. Several ob-

https://doi.org/10.5194/egusphere-2026-4390
Preprint. Discussion started: 4 August 2026

servations are assimilated, such as along-track altimeter data, satellite sea surface temperature, and in situ data for temperature and salinity. The data are delivered as daily and monthly mean fields.

The real-time drifter data are provided by the Observing System Monitoring Center (OSMC, https://osmc.noaa.gov/erddap/tabledap/OSMC_flattened.html, last access: 2 March 2026) and are part of the Global Drifter Program (GDP) funded by the National Oceanic and Atmospheric Administration (NOAA). The surface velocity program (SVP) drifters that were deployed during the research cruise MSM117 were also part of the GDP. They are equipped with a surface float measuring 35 cm in diameter, and a holey sock drogue that enables the drifters to drift with the upper 15 m ocean currents (Lopez et al., 2014). Iridium short burst data telemetry for satellite transmission enables the drifter to send its position and sea surface temperature data, usually once per hour. The data are then available in near-real time. The accuracy of the position ranges from about 2-50 m. The lifetime is about two years, depending on the sampling and transmission rate. The unique World Meteorological Organization (WMO) numbers of the three deployed drifters are listed in Figure 2. The climatology for the global near-surface drifter-derived currents is provided by the Physical Oceanography Division of the National Oceanic and Atmospheric Administration/Atlantic Oceanographic and Meteorological Laboratory (NOAA/AOML, Laurindo et al. (2017)). We used version 3.10, which was last updated in August 2023 (https://www.aoml.noaa.gov/phod/gdp/mean_velocity.php, last access: 30 June 2026).

In situ measurements of horizontal velocities by a moored observatory that is part of the Prediction and Research Moored Array in the Tropical Atlantic (PIRATA) at 23 °W and 0 ° were used (Tuchen et al., 2023). This array measured current velocities for the past 20 years and therefore provides a good reference dataset (Tuchen et al., 2022a). This dataset combines measurements from a surface buoy with moored subsurface measurements. The velocities are given in meters per second.

2.2 Methods

2.2.1 Yanai Wave Velocities

To investigate the influence of a 14-day Yanai wave on the velocity field in the region, equations for the meridional and zonal wave velocities are derived. Furthermore, the trajectories of a hypothetical drifter following these velocities, in addition to a climatological background field, are calculated.

To describe motions on the equatorial β-plane, a common approach is to use the linearized, gravity-reduced shallow water equations (e.g. Matsuno, 1966; McCreary, 1984; Holton, 2004). From these equations, the dispersion relation for Yanai waves can be determined:

$$\frac{\omega}{c} - k - \frac{\beta}{\omega} = 0 \tag{1}$$

where k is the zonal wave number, ω is the wave frequency, β is the meridional gradient of the Coriolis parameter, $c = 1.3$ $\mathrm{m\,s^{-1}}$ is the gravity wave speed of the second baroclinic mode (Gill, 1982). A period of 14 days corresponds to a wavelength of $\lambda = \frac{2\pi}{k} \approx 14500$ km or about 110 ° longitude.

https://doi.org/10.5194/egusphere-2026-4390
Preprint. Discussion started: 4 August 2026

From the dispersion relation (1), one can derive equations for the zonal (u) and meridional (v) velocities (Gill, 1982):

$$u_{Yanai} = -\frac{\omega y}{c} A e^{\frac{-\beta y^2}{2c}} \sin(kx - \omega t) \tag{2}$$

$$v_{Yanai} = A e^{\frac{-\beta y^2}{2c}} \cos(kx - \omega t). \tag{3}$$

The amplitude A of the Yanai wave is estimated by the cross-equatorial drift velocity of the real drifters (0.4-0.7 $\mathrm{m\,s^{-1}}$). We use these velocity equations for the artificial drifter experiments to analyze the influence of the Yanai wave on surface velocities in the western equatorial Atlantic.

2.2.2 Artificial Drifter Trajectories

In order to investigate whether Yanai waves can cause surface currents contributing to circular motion centered at the equator, we conduct a series of numerical experiments. In these experiments, artificial drifters are deployed in a velocity field that combines both a climatological background field from NOAA/AOML (see above) and velocities associated with Yanai waves (Eq. 3). The trajectories of the artificial drifters are then calculated as follows:

$$x(i+1) = x(i) + \{u_{Yanai}(x(i), y(i)) + u_{Background}(x(i), y(i))\} \cdot dt \tag{4}$$

$$y(i+1) = x(i) + \{v_{Yanai}(x(i), y(i)) + v_{Background}(x(i), y(i))\} \cdot dt. \tag{5}$$

$x(i+1)$ and $y(i+1)$ represent the longitude and latitude of the current position, while $x(i)$ and $y(i)$ represent the previous position. Initially, at $i = 0$, $x(i) = x(0)$ and $y(i) = y(0)$ denote the starting positions. u_{Yanai}, v_{Yanai} and $u_{background}$, $v_{background}$ represent the velocities of the Yanai wave field (see Eq. 3) and the background current field at $x(i)$ and $y(i)$, respectively. The time step, denoted by dt, is chosen to be 20 minutes to ensure a smooth trajectory.

2.2.3 Bandpass filtering

In order to check for the presence of Yanai waves, we analyze the cross-equatorial wind fluctuations, which constitute an established generation mechanism. To highlight the biweekly fluctuations, we bandpass-filter the meridional wind component at periods close to the observed 14 days. To determine the exact cut-off periods for the bandpass filter, the power spectral density (PSD) is calculated. The data is pre-processed using a Hann window function to minimize spectral leakage. The Hann window is a widely used window for time series analysis (e.g. Körner et al., 2022) and is defined by $w(n) = 0.5 - 0.5\cos(\frac{2\pi n}{M-1})$ for $0 \leq n \leq M-1$. Local minima surrounding the 14-day period are chosen as cut-off periods for the bandpass filter. For the meridional wind data, the local minima correspond to 11 and 20 days. For the bandpass filter, an 8th order Butterworth filter is used. The same method and cut-off periods are applied to the surface current data. The functions used for the PSD and the bandpass filter originate from the Python scipy package (Virtanen et al., 2020).

2.2.4 Validation of reanalysis products

Reanalysis products consist of several sources, including a baseline model and assimilated remote sensing or in situ data. To assess how well they represent our study region, we compare different quantities to in situ measurements from the moored

https://doi.org/10.5194/egusphere-2026-4390
Preprint. Discussion started: 4 August 2026

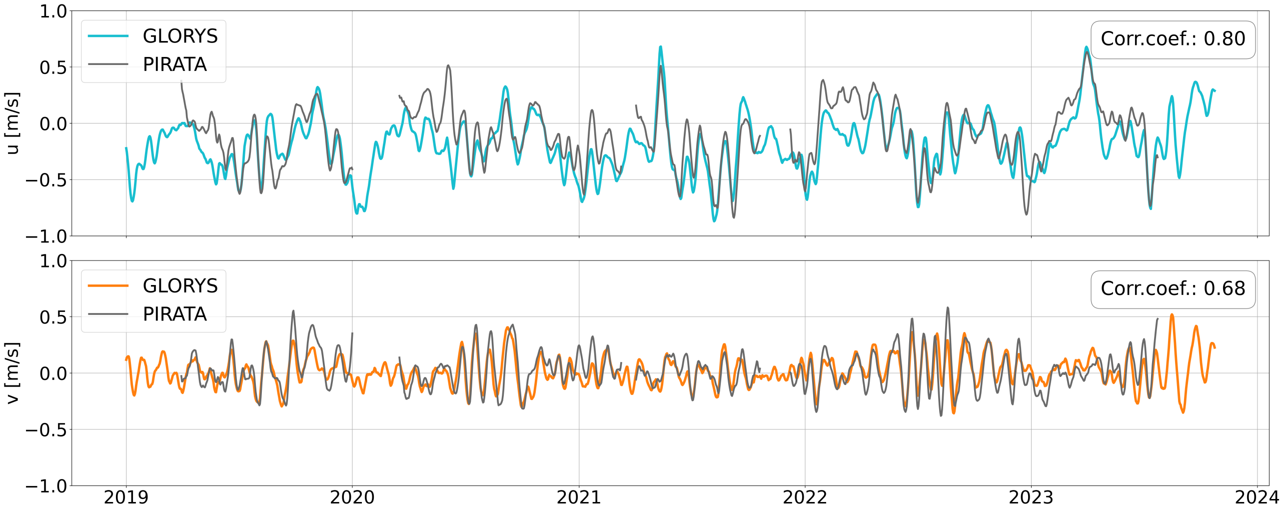

Figure 1. Comparison of upper 15 m zonal (upper panel) and meridional (lower panel) velocities for GLORYS (cyan/orange) and PIRATA (black) at the equator and 23 °W for 2019-2024 filtered by a 10-day running mean. The Pearson correlation coefficient is calculated for each panel (unitless). Velocities are given in meters per second.

PIRATA array located at 23 °W and at the equator (Fig. 1). Both datasets are averaged over the upper 15 m and smoothed with a 10-day running mean. For the comparison of the velocities, output from GLORYS reanalysis is selected at the same location as the PIRATA buoy. Note that the PIRATA dataset does not cover the full time period. The Pearson correlation coefficient is calculated as follows, utilizing the pandas toolbox (McKinney, 2010; The pandas development Team, 2020):

$$r = \frac{\sum(x-m_x)(y-m_y)}{\sqrt{\sum(x-m_x)^2\sum(y-m_y)^2}} \quad (6)$$

where m_x and m_y are the means of the vectors x and y that are to be correlated, respectively. The Pearson correlation coefficient shows values of 0.8 (0.68) for the zonal (meridional) velocity component. Therefore, we trust the reanalysis dataset to reproduce the surface velocities at the equator.

3 Results

3.1 Observations

During the research cruise MSM117 eight SVP drifters were deployed in May 2023 off Brazil at 35 °W between 0-2.5 °S. Five drifters followed the coastline northwestward, driven by the NBC. The remaining three drifters were accelerated out of the mean northwestward flow and completed one to two cycles centered at the equator. The period of all three drifters was 14 days regardless of the individual diameters of the circles. The diameters ranged from 61 km to 138 km (orange and green colors in Fig. 2, respectively).

https://doi.org/10.5194/egusphere-2026-4390
Preprint. Discussion started: 4 August 2026

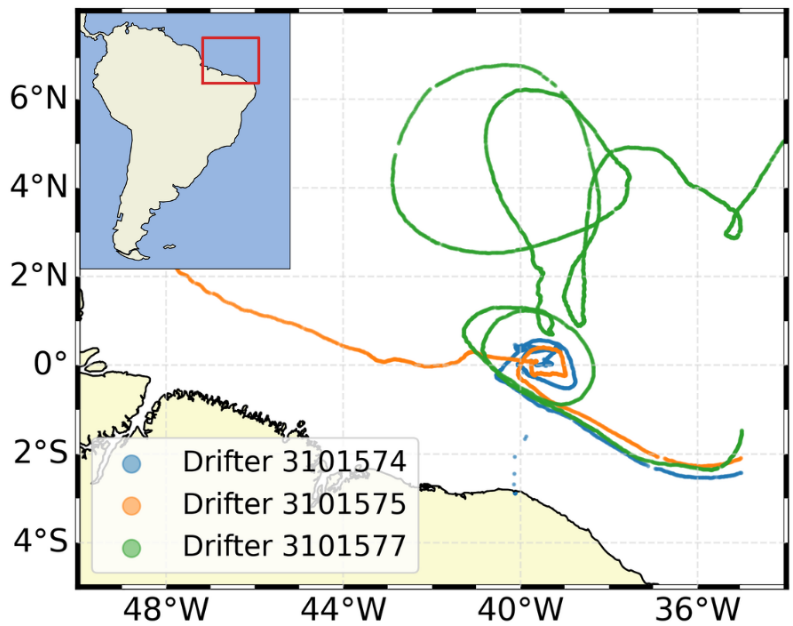

Figure 2. Trajectories of surface drifters deployed in May 2023 at 35 °W during the research cruise MSM117 and their unique WMO numbers. Map of South America with a red box indicating the area of interest.

To investigate whether Lagrangian drifters can be used to observe and describe Yanai waves and whether the circular trajectories at the equator can be partly attributed to a Yanai wave, we took the following three steps. First, we analyzed wind data to examine if the atmospheric forcing needed to generate a Yanai wave was present. Second, we used surface current data from a reanalysis product to find further evidence for the existence of a Yanai wave. Last, we conducted a series of experiments with artificial drifters to reproduce the observed situation.

3.2 Generation Mechanism

We focus on the generation mechanism of biweekly Yanai waves to test whether the theoretical conditions for this wave were present in May to July, 2023. Biweekly Yanai waves in the ocean can be generated (besides other mechanisms) by cross-equatorial wind fluctuations. In order to focus on the biweekly fluctuations in the meridional wind component, we bandpass-filtered the meridional wind data between 11 and 20 days. The region was chosen centered about 40 °W from 35 °W to 45 °W and 1.5 °N to 1.5 °S. A Hovmöller diagram of the meridional averaged and bandpass-filtered wind data reveals a strong biweekly periodicity (colors in Fig. 3). This signal is especially strong during May, one month before the observed circular motion of the drifters. These biweekly meridional wind fluctuations resemble the atmospheric forcing needed to generate a 14-day Yanai wave.

https://doi.org/10.5194/egusphere-2026-4390
Preprint. Discussion started: 4 August 2026

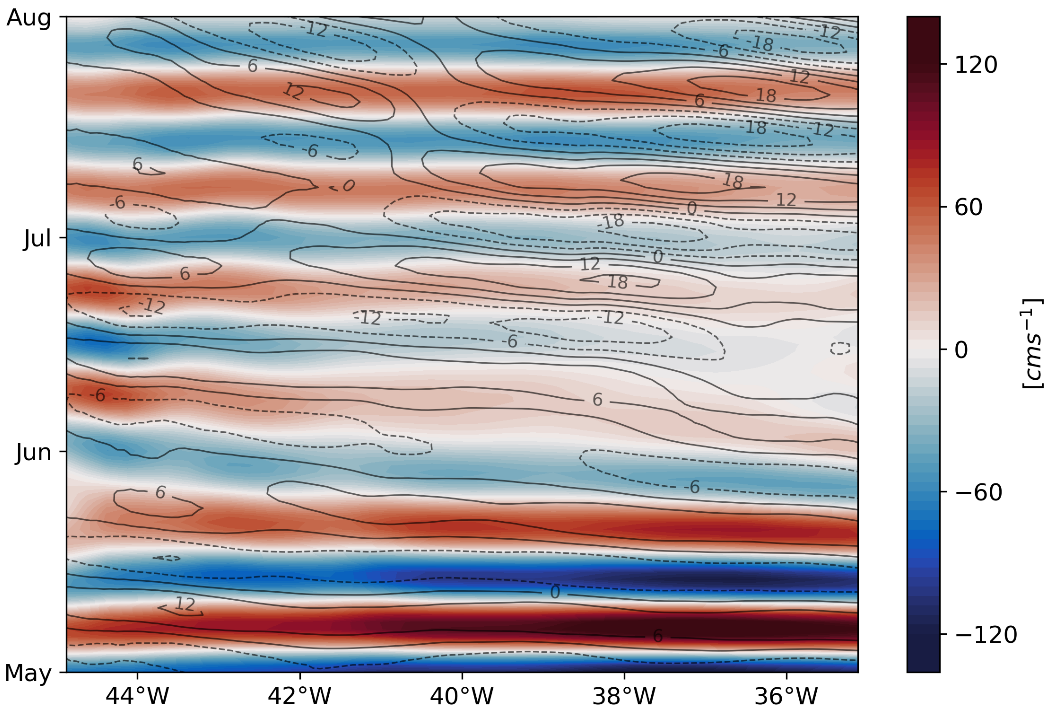

Figure 3. Hovmöller diagram: bandpass-filtered meridional wind speed (10 m) for 11-20 days averaged within ±1.5 ° latitude of the equator. Red (blue) values represent northward (southward) velocities. Solid (dashed) black lines indicate contour lines of positive/northward (negative/southward) meridional current velocities (upper 15 m) filtered for the same period and area. All velocities are given in centimeters per second.

3.3 Surface Current Analysis

To further confirm the presence of a 14-day Yanai wave, we analyze the upper ocean currents for a signal in the meridional velocity component. Usually, Yanai waves in the ocean are described using observational data from current meters or moored acoustic Doppler current profilers. Unfortunately, in the area of interest close to 40 °W, no moorings, buoys, or other suitable observational platforms were present. We thus applied the same technique used for the wind data to the averaged upper 15 m velocities from the GLORYS reanalysis data product. The cut-off periods chosen for the bandpass filter were set to same periods as for the wind data 11 to 20 days. Similar to the wind data, the filtered meridional current velocities show strong fluctuations increasing mid-June and during July, supporting the theory of a Yanai wave during that time (contour lines in Fig. 3). In conclusion, we find indicators for the presence of a 14-day Yanai wave in the ocean based on biweekly fluctuations in the meridional wind and surface current components.

https://doi.org/10.5194/egusphere-2026-4390
Preprint. Discussion started: 4 August 2026

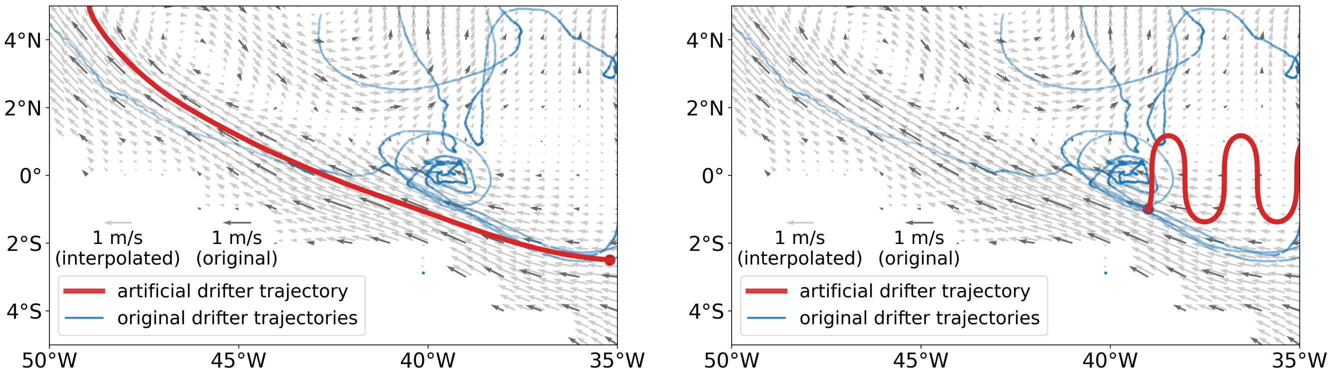

Figure 4. Artificial drifter trajectories (red) with, left panel: only climatological drifter-derived near-surface velocity field, right panel: only Yanai wave-associated velocities are included. Dark (light) grey arrows represent the original (interpolated) climatological field. Blue lines show the original drifter trajectories.

3.4 Artificial Drifter Experiments

Since signals in cross-equatorial wind and current velocities indicate the presence of a Yanai wave, we conducted a series of numerical experiments to show that by using velocities of a Yanai wave combined with the background flow field from NOAA/AOML, a situation observed by three SVP drifters in boreal summer 2023 in the western equatorial Atlantic can be reproduced. The experiments produced trajectories of artificial ocean surface drifters floating in a velocity field that combines both a steady state climatological estimate and velocities that are derived from a 14-day Yanai wave.

The goal is to demonstrate two things, first that ocean drifters can be used to observe and describe Yanai waves, and second that Yanai wave-associated surface velocities can contribute to circular trajectories at the equator in the Western Atlantic. Therefore, the experiments with artificial drifters were conducted to reproduce the situation using Yanai wave velocities. A set of artificial drifters was deployed close to the real deployment positions during the cruise. Half of the observed circular motion was positioned within the NBC, while the other half of the circles was completed against the mean current. The prevailing winds were aligned with the NBC, and possibly also contributed to the motion of the drifters.

However, the design of the drifters with an underwater drogue, centered at 15 m depth, is intended to ensure that the drifters are mainly driven by currents rather than winds. Therefore, we attribute the full circle to the combination of a strong northwestward current, the NBC, and the velocities associated with a Yanai wave. We found that neither of the two factors alone was able to reproduce the situation (Fig. 4). The period of the Yanai wave was set to 14 days because the SVP drifters all took 14 days to complete one circle. Once deployed, we monitored the trajectories of the artificial drifters. Throughout the experiment, the initial conditions were varied (Table 1). These parameters include the amplitude and phase of the Yanai wave, the background velocity field, and the initial position of the artificial drifters.

We chose to deploy the artificial drifters in two different locations, one very close to 40 °W where the SVP drifters circled, whereas the second location resembles the original deployment locations along 35 °W. In the following, they will be referred

https://doi.org/10.5194/egusphere-2026-4390
Preprint. Discussion started: 4 August 2026

Parameter	Description / Range
Wave amplitude (A)	0.5-0.7 $\mathrm{m\,s^{-1}}$
Wave phase	0-2 π in steps of $\frac{\pi}{4}$
Deployment position:	
Latitudes ($y(0)$)	0.5 °N-2.5 °S
Longitudes ($x(0)$)	35 °W, 38.5-41 °W
Background field	Monthly climatological currents derived from drifter data for May, June, and July.

Table 1. Parameters and corresponding ranges of initial conditions that were varied throughout the experiment with artificial drifters.

to as 40 °W- and 35 °W-experiment, respectively. Varying initial conditions in both experiments led to a total number of 1.881 deployed artificial drifters (40 °W: 1447, 35 °W: 434). By looking at each plot individually, the behavior of artificial drifters is divided into two main categories: those that mimic the observed motion and those that either do not circle at all or do not circle at the equator in the specific area. The latter is further divided into five groups based on the most common trajectory shapes (Fig. 5):

- East: This group contains drifters deployed in the 35 °W-experiment that either never enter the plotted area or only slightly, indicating an eastward drift. This behavior is unique to this experiment since the deployment location in the other experiment is always further to the west.
- Coast: Drifters in this group head directly to the coast or initially move outside the plotted area before ending up at the coast.
- North: Drifters categorized in this group come close to the circling area but either head directly northward, fail to complete the circle, circle at a distance from the area, or complete a very small circle.
- NBC: This group is further divided into two subgroups:
  - NBC without circle: Trajectories in this subgroup follow the NBC without completing any circling motion.
  - NBC with circle: This sub-group includes drifters that also follow the NBC but exhibit some circling behavior along the way, although not close to the area of interest or only very small circles.

Regardless of the experiment, about 80 % of the artificial drifters did not show circular trajectories. Only about 10 % of all cases showed trajectories that resemble the observed pathways (Fig. 6). In the following, we will focus on the trajectories that reproduced the observed situation. This group contains 179 (40) cases for the 40 °W (35 °W) experiment. To understand which initial conditions lead to the reproduction of the situation, we compared the different values of the initial conditions and their success rate (number of deployments that result in trajectories similar to observations, Fig. 7). For both experiments, a similar behavior is observed for the variation of the amplitude of the Yanai wave and the month for the climatological background

https://doi.org/10.5194/egusphere-2026-4390
Preprint. Discussion started: 4 August 2026

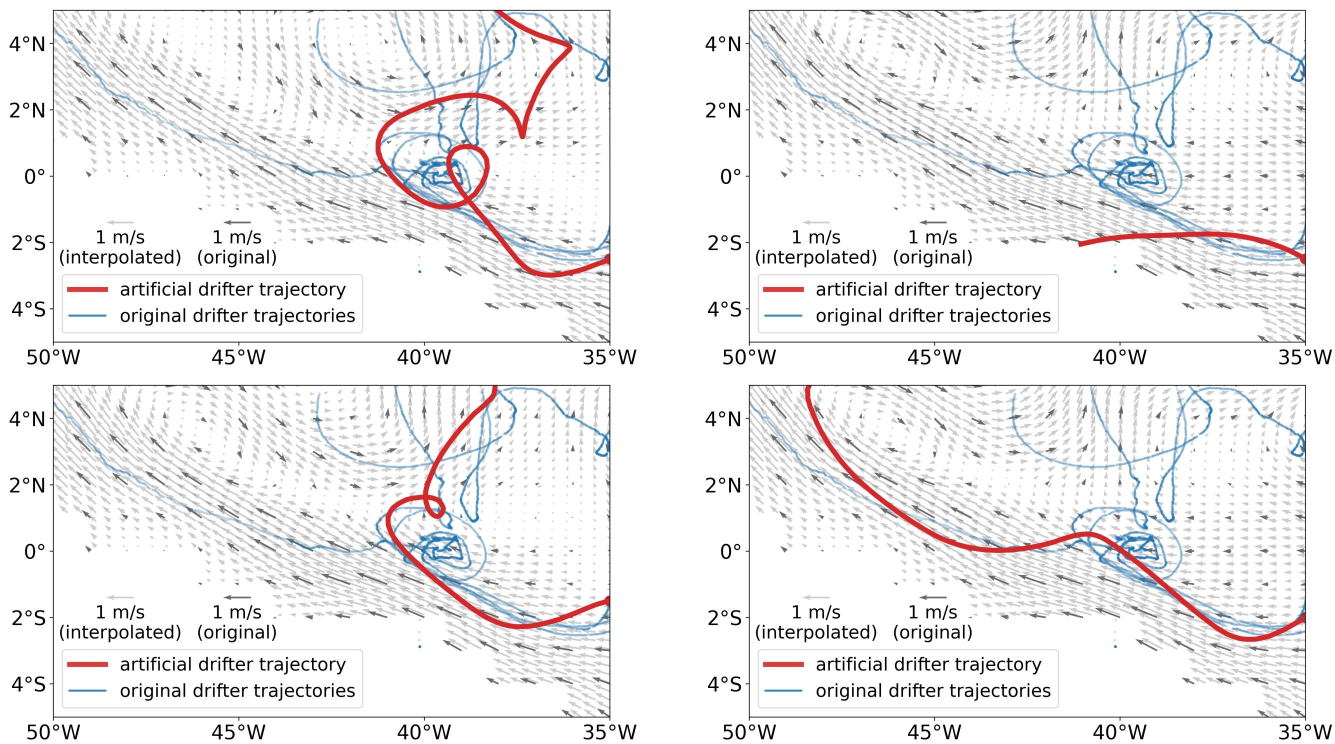

Figure 5. Categories for artificial drifter trajectories (red) with a climatological drifter-derived near-surface velocity field. Dark (light) grey arrows represent the original (interpolated) field. Blue colors show the original drifter trajectories. Top left: reality-close group, top right: coast-group, bottom left: north-group, bottom right: NBC-group.

field: Larger amplitudes and climatological background velocity field for May and June are more likely to lead to reality-close trajectories than smaller amplitudes and those for July. The variation of the deployment position along latitudes is not as straightforward. Deployment positions south of the equator seem to produce more often reality-close trajectories than those close or north of the equator. But the results contain a bias towards latitudes south of the equator because during the 35 °W experiment, only latitudes of 0 to 2.5 °S were used. The variation of the phase of the Yanai wave also shows different results for the two experiments. The phase of the Yanai wave can be adjusted by adding a value to the $\cos(kx - wt{+}\text{phase})$ and $\sin(kx - wt{+}\text{phase})$ terms used in the calculation of the velocities of Yanai waves (Eq. 3). During the 40 °W experiment (35 °W experiment), periods of 0, $\frac{1}{4}\pi$ and $\frac{3}{4}\pi$ ($1\frac{1}{4}\pi$ and $1\frac{1}{2}\pi$) are more likely to produce reality-close trajectories. These differences can be explained by the different longitudinal deployment positions and the time the artificial drifters need to enter the area. The meridional velocities induced by a Yanai wave are not symmetric about the equator leading to cross-equatorial velocities. These alternate between northward and southward velocities. Phases of 0, $\frac{1}{4}\pi$, and $\frac{1}{2}\pi$ generate northward velocities at the equator. Trajectories in the 40 °W experiments were more likely close to reality when the phase of the Yanai wave was set

https://doi.org/10.5194/egusphere-2026-4390
Preprint. Discussion started: 4 August 2026

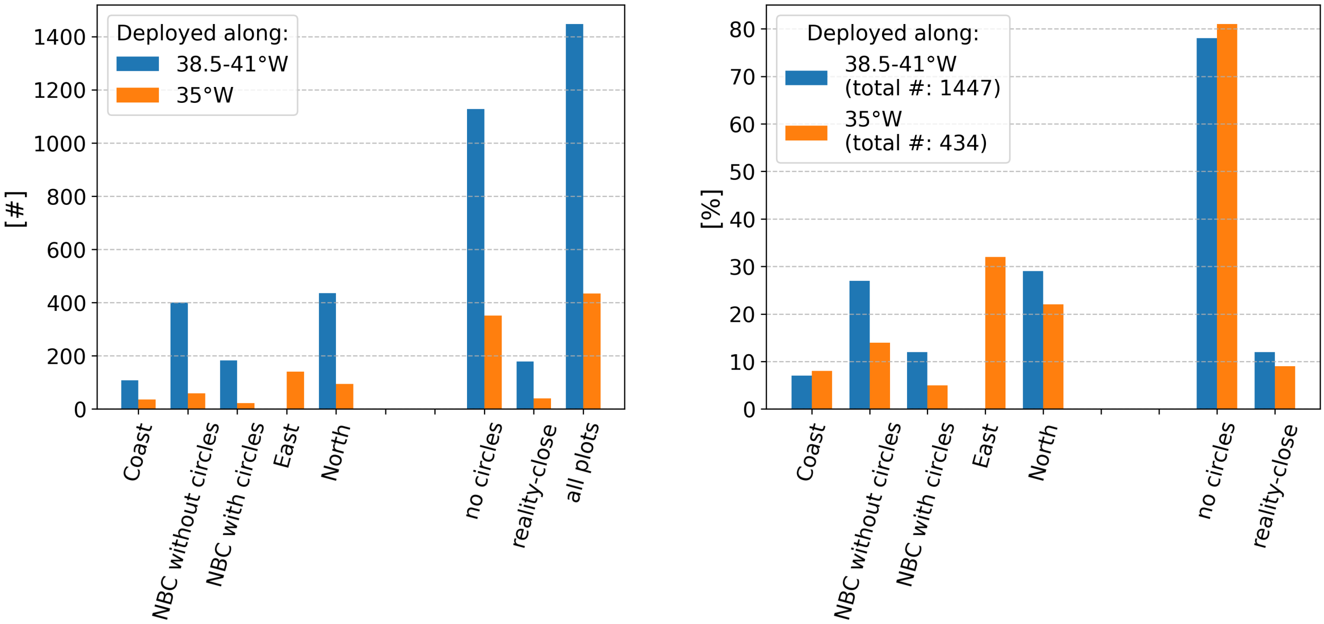

Figure 6. Categories for artificial drifter trajectories (Coast, NBC with and without circles, East, and North) in total numbers (left panel) and percentage regarding the total amount of plots of each experiment (right panel). Colors stand for the 40 °W (blue) and the 35 °W (orange) experiment. Furthermore, the total number of plots generated in the experiment is shown, the number of reality-close circles and plots without circles.

initially to one of these. In this experiment, the drifters were deployed directly in the region where the SVP drifters circled, the northward velocities of the Yanai wave steered the artificial drifters northward away from the strong NBC. The artificial drifters in the 35 °W experiment were deployed further to the east. Hence, they needed time to reach the area where the SVP drifter circled. During this time, the Yanai wave also evolved. For the Yanai wave to produce northward velocities when artificial drifters reached the area, the initial phase needed to be a southward phase (i.e. $1\frac{1}{4}\pi$, $1\frac{1}{2}\pi$).

Even though this is quite a unique case-study, the concept of using Lagrangian surface drifter data to identify Yanai waves in regions with sparse observational data could be useful in the future. This is important because they contribute to intraseasonal variability, mixing in the mid-depth and deep ocean, and the large-scale circulation through their interactions and dissipation (e.g. Greatbatch et al., 2018; Nagura and McPhaden, 2024). Therefore, a better understanding of these processes will improve model performance and, ultimately, weather and climate predictions.

4 Conclusions

Motivated by three SVP drifters that experienced circular trajectories in boreal summer 2023, we investigated if this behavior can be partly attributed to the presence of Yanai waves in the western equatorial Atlantic. Both meridional wind and surface

https://doi.org/10.5194/egusphere-2026-4390
Preprint. Discussion started: 4 August 2026

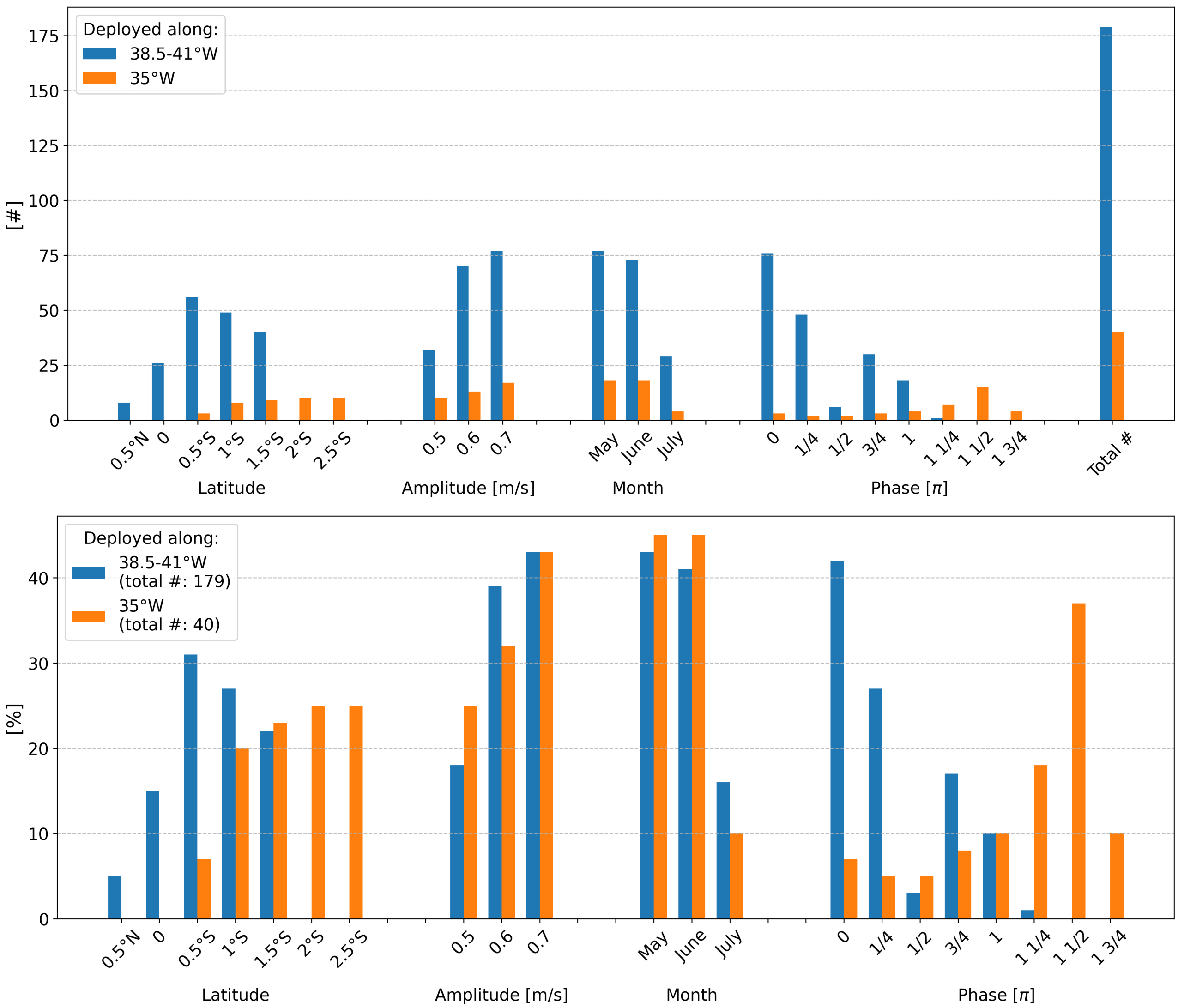

Figure 7. Distribution of initial conditions among the group of reality-close circles for each experiment (blue: 40 °W, orange: 35 °W). The upper (lower) panel shows total numbers (percentage of all reality-close circles) for each category. Latitude denotes the deployment latitude, amplitude and phase are characteristics of the Yanai wave. Month indicates the month chosen for the climatological background velocity field. Total # represents the total number of plots generated in each experiment.

current data showed conditions favorable for the generation and presence of a biweekly Yanai wave. Experiments with artificial drifters that were deployed in a velocity field containing a biweekly Yanai wave, showed that circular trajectories are reproducible. Hence, ocean surface drifters can be used to track and analyze oceanic Yanai waves, and these waves can cause these drifters to circle at the equator (under certain conditions, i.e. strong coastal NBC).

https://doi.org/10.5194/egusphere-2026-4390
Preprint. Discussion started: 4 August 2026

Trajectories of waves at the equator have rarely been observed because of the predominant dynamics that cause floating instruments to quickly drift to higher latitudes. To our knowledge, this is the first description of directly observed Yanai wave trajectories in the Atlantic. Furthermore, Yanai waves have been described quite frequently for the eastern part of the Atlantic basin, but less so far west as 40 °W.

The observed situation is quite unique. A set of various conditions contributed to the observed situation: The timing of wind fluctuations, drifter deployment positions, phase and amplitude of the Yanai wave, and the precise position and strength of the NBC. Consequently, it may prove challenging to replicate or re-observe such behavior in the future. While a comprehensive deployment of surface drifters in boreal summer, particularly close to 40 °W, could potentially yield results, the probability of success remains low (the experiments showed only a success rate of about 10 %).

However, in future research, drifter data can be taken into account to analyze Yanai waves in other regions or ocean basins. Drifters are less constrained compared to, for example, moored instruments, and as the fleet of ocean drifters steadily increases, they will provide a wide range of potentially interesting and useful data. Nevertheless, the drift to higher latitudes due to poleward Ekman flow remains a drawback for this method. However, drifters that are deployed close to or at the equator might be able to collect valuable data before they are dislocated towards higher latitudes. Due to the period of about two weeks, shipboard measurements seem unlikely to give further insights, because research vessels rarely stay in the same area for several weeks. Additionally, the attempt of this study to reconstruct the situation using a background velocity field, along with the velocities of a Yanai wave, remains somewhat simplistic. An alternative approach could involve utilizing a more complex coupled ocean-atmosphere model instead of relying solely on a climatological background field. In such a setup, the wind forcing could be manipulated and experimented with. The behavior of the artificial drifter, with or without the initial wind forcing, as well as the optimal timing of such forcing, could be analyzed. Furthermore, the conditions needed to best replicate the situation could be refined by deliberately generating specific Yanai waves at desired locations.

Author contributions. Conceptualization, design, and methodology: all authors. Data analysis, simulations, and preparation of the first draft of the manuscript: AA. Reviewing, editing, and correcting of the manuscript: all authors.

Competing interests. The authors declare that they have no conflict of interest.

Acknowledgements. This research was partly funded by the European Space Agency through the Upper Ocean Dynamics project (ESA Contract No. 4000146102/24/I-EB). This study used observations from the Global Drifter Program collected and distributed by NOAA's Atlantic Oceanographic and Meteorological Laboratory.

https://doi.org/10.5194/egusphere-2026-4390
Preprint. Discussion started: 4 August 2026

References

Aguedjou, H. M. A., Dadou, I., Chaigneau, A., Morel, Y., and Alory, G.: Eddies in the Tropical Atlantic Ocean and Their Seasonal Variability, Geophysical Research Letters, 46, 12 156–12 164, https://doi.org/10.1029/2019GL083925, 2019.

Braga, H. A. and Magaña, V.: Atmospheric Mixed Rossby–Gravity Waves over the Tropical Pacific during the Austral Summer, Weather and Climate Dynamics, 6, 265–277, https://doi.org/10.5194/wcd-6-265-2025, 2025.

Chatterjee, A., Shankar, D., McCreary Jr., J., and Vinayachandran, P. N.: Yanai Waves in the Western Equatorial Indian Ocean, Journal of Geophysical Research: Oceans, 118, 1556–1570, https://doi.org/10.1002/jgrc.20121, 2013.

David, D. T., Kumar, S. P., Byju, P., Sarma, M. S. S., Suryanarayana, A., and Murty, V. S. N.: Observational Evidence of Lower-Frequency Yanai Waves in the Central Equatorial Indian Ocean, Journal of Geophysical Research: Oceans, 116, https://doi.org/10.1029/2010JC006603, 2011.

Farrar, J. T. and Durland, T. S.: Wavenumber–Frequency Spectra of Inertia–Gravity and Mixed Rossby–Gravity Waves in the Equatorial Pacific Ocean, Journal of Physical Oceanography, 42, 1859–1881, https://doi.org/10.1175/JPO-D-11-0235.1, 2012.

Gill, A.: Atmosphere-Ocean Dynamics, International Geophysics Series, Academic Press, ISBN 978-0-12-283520-9, 1982.

Greatbatch, R. J., Claus, M., Brandt, P., Matthießen, J.-D., Tuchen, F. P., Ascani, F., Dengler, M., Toole, J., Roth, C., and Farrar, J. T.: Evidence for the Maintenance of Slowly Varying Equatorial Currents by Intraseasonal Variability, Geophysical Research Letters, 45, 1923–1929, https://doi.org/10.1002/2017GL076662, 2018.

Holton, J. R.: An Introduction to Dynamic Meteorology, no. v. 88 in International Geophysics Series, Elsevier Academic Press, Burlington, MA, 4th edition edn., ISBN 978-0-12-354015-7, 2004.

Jean-Michel, L., Eric, G., Romain, B.-B., Gilles, G., Angélique, M., Marie, D., Clément, B., Mathieu, H., Olivier, L. G., Charly, R., Tony, C., Charles-Emmanuel, T., Florent, G., Giovanni, R., Mounir, B., Yann, D., and Pierre-Yves, L. T.: The Copernicus Global 1/12° Oceanic and Sea Ice GLORYS12 Reanalysis, Frontiers in Earth Science, 9, https://doi.org/10.3389/feart.2021.698876, 2021.

Jochum, M. and Malanotte-Rizzoli, P.: On the Generation of North Brazil Current Rings, Journal of Marine Research, 61, 147–173, https://doi.org/10.1357/002224003322005050, 2003.

Körner, M., Claus, M., Brandt, P., and Tuchen, F. P.: Sources and Pathways of Intraseasonal Meridional Kinetic Energy in the Equatorial Atlantic Ocean, Journal of Physical Oceanography, 52, 2445–2462, https://doi.org/10.1175/JPO-D-21-0315.1, 2022.

Laurindo, L. C., Mariano, A. J., and Lumpkin, R.: An Improved Near-Surface Velocity Climatology for the Global Ocean from Drifter Observations, Deep Sea Research Part I: Oceanographic Research Papers, 124, 73–92, https://doi.org/10.1016/j.dsr.2017.04.009, 2017.

Lopez, R., Malardé, J.-P., Royer, F., and Gaspar, P.: Improving Argos Doppler Location Using Multiple-Model Kalman Filtering, IEEE Transactions on Geoscience and Remote Sensing, 52, 4744–4755, https://doi.org/10.1109/TGRS.2013.2284293, 2014.

Luyten, J. R. and Roemmich, D. H.: Equatorial Currents at Semi-Annual Period in the Indian Ocean, Journal of Physical Oceanography, 12, 406–413, https://doi.org/10.1175/1520-0485(1982)012<0406:ECASAP>2.0.CO;2, 1982.

Magaña, V. and Yanai, M.: Mixed Rossby–Gravity Waves Triggered by Lateral Forcing, Journal of the Atmospheric Sciences, 52, 1473–1486, https://doi.org/10.1175/1520-0469(1995)052<1473:MRWTBL>2.0.CO;2, 1995.

Matsuno, T.: Quasi-Geostrophic Motions in the Equatorial Area, Journal of the Meteorological Society of Japan. Ser. II, 44, 25–43, https://doi.org/10.2151/jmsj1965.44.1_25, 1966.

McCreary, Jr., J. P.: Equatorial Beams, Journal of Marine Research, 42, 395–430, https://doi.org/10.1357/002224084788502792, 1984.

https://doi.org/10.5194/egusphere-2026-4390
Preprint. Discussion started: 4 August 2026

McKinney, W.: Data Structures for Statistical Computing in Python, in: Proceedings of the 9th Python in Science Conference, edited by van der Walt, S. and Millman, J., pp. 56–61, https://doi.org/10.25080/Majora-92bf1922-00a, 2010.

McPhaden, M. J. and Picaut, J.: El Niño-Southern Oscillation Displacements of the Western Equatorial Pacific Warm Pool, Science, 250, 1385–1388, https://doi.org/10.1126/science.250.4986.1385, 1990.

Mears, C., Lee, T., Ricciardulli, L., Wang, X., and Wentz, F.: RSS Cross-Calibrated Multi-Platform (CCMP) 6-Hourly Ocean Vector Wind Analysis on 0.25 Deg Grid, Version 3.0, https://doi.org/10.56236/RSS-uv6h30, 2022.

Nagura, M. and McPhaden, M. J.: Dual-Frequency Wind-Driven Mixed Rossby–Gravity Waves in the Equatorial Indian Ocean, Journal of Physical Oceanography, 53, 1535–1553, https://doi.org/10.1175/JPO-D-22-0222.1, 2023.

Nagura, M. and McPhaden, M. J.: Mixed Rossby Gravity Waves at Middepths of the Equatorial Indian Ocean, Journal of Physical Oceanography, 54, 1787–1805, https://doi.org/10.1175/JPO-D-23-0254.1, 2024.

Schott, F. A. and McCreary, J. P.: The Monsoon Circulation of the Indian Ocean, Progress in Oceanography, 51, 1–123, https://doi.org/10.1016/S0079-6611(01)00083-0, 2001.

Schott, F. A., Fischer, J., and Stramma, L.: Transports and Pathways of the Upper-Layer Circulation in the Western Tropical Atlantic, Journal of Physical Oceanography, 28, 1904–1928, https://doi.org/10.1175/1520-0485(1998)028<1904:TAPOTU>2.0.CO;2, 1998.

Sengupta, D., Senan, R., and Goswami, B. N.: Origin of Intraseasonal Variability of Circulation in the Tropical Central Indian Ocean, Geophysical Research Letters, 28, 1267–1270, https://doi.org/10.1029/2000GL012251, 2001.

Shinoda, T.: Observation of First and Second Baroclinic Mode Yanai Waves in the Ocean, Quarterly Journal of the Royal Meteorological Society, 138, 1018–1024, https://doi.org/10.1002/qj.968, 2012.

Takasuka, D. and Satoh, M.: Dynamical Roles of Mixed Rossby–Gravity Waves in Driving Convective Initiation and Propagation of the Madden–Julian Oscillation: General Views, Journal of the Atmospheric Sciences, 77, 4211–4231, https://doi.org/10.1175/JAS-D-20-0050.1, 2020.

Terada, Y. and Masumoto, Y.: Origin of the Intraseasonal Current Variability and Its Interannual Modulation at 1,000 m Depth in the Eastern Equatorial Pacific Ocean, Journal of Geophysical Research: Oceans, 130, e2025JC022 754, https://doi.org/10.1029/2025JC022754, 2025.

The pandas development Team: Pandas-Dev/Pandas: Pandas (Version v3.0.4) [Computer software], Zenodo, https://doi.org/10.5281/zenodo.3509134, 2020.

Tuchen, F. P., Brandt, P., Claus, M., and Hummels, R.: Deep Intraseasonal Variability in the Central Equatorial Atlantic, Journal of Physical Oceanography, 48, 2851–2865, https://doi.org/10.1175/JPO-D-18-0059.1, 2018.

Tuchen, F. P., Lübbecke, J. F., Brandt, P., and Fu, Y.: Observed Transport Variability of the Atlantic Subtropical Cells and Their Connection to Tropical Sea Surface Temperature Variability, Journal of Geophysical Research: Oceans, 125, e2020JC016 592, https://doi.org/10.1029/2020JC016592, 2020.

Tuchen, F. P., Brandt, P., Hahn, J., Hummels, R., Krahmann, G., Bourlès, B., Provost, C., McPhaden, M. J., and Toole, J. M.: Two Decades of Full-Depth Current Velocity Observations from a Moored Observatory in the Central Equatorial Atlantic at 0°N, 23°W, Frontiers in Marine Science, 9, https://doi.org/10.3389/fmars.2022.910979, 2022a.

Tuchen, F. P., Brandt, P., Lübbecke, J. F., and Hummels, R.: Transports and Pathways of the Tropical AMOC Return Flow From Argo Data and Shipboard Velocity Measurements, Journal of Geophysical Research: Oceans, 127, e2021JC018 115, https://doi.org/10.1029/2021JC018115, 2022b.

Tuchen, F. P., Brandt, P., Hahn, J., Hummels, R., Krahmann, G., Bourles, B., Provost, C., McPhaden, M. J., and Toole, J. M.: Data Product of Full-Depth Current Velocity Observations at 0°N, 23°W from 2001-2023 (v2.0), https://doi.org/10.1594/PANGAEA.963935, 2023.

https://doi.org/10.5194/egusphere-2026-4390
Preprint. Discussion started: 4 August 2026

Virtanen, P., Gommers, R., Oliphant, T. E., Haberland, M., Reddy, T., Cournapeau, D., Burovski, E., Peterson, P., Weckesser, W., Bright, J., van der Walt, S. J., Brett, M., Wilson, J., Millman, K. J., Mayorov, N., Nelson, A. R. J., Jones, E., Kern, R., Larson, E., Carey, C. J., Polat, İ., Feng, Y., Moore, E. W., VanderPlas, J., Laxalde, D., Perktold, J., Cimrman, R., Henriksen, I., Quintero, E. A., Harris, C. R., Archibald, A. M., Ribeiro, A. H., Pedregosa, F., and van Mulbregt, P.: SciPy 1.0: Fundamental Algorithms for Scientific Computing in Python, Nature Methods, 17, 261–272, https://doi.org/10.1038/s41592-019-0686-2, 2020.

von Schuckmann, K., Brandt, P., and Eden, C.: Generation of Tropical Instability Waves in the Atlantic Ocean, Journal of Geophysical Research: Oceans, 113, https://doi.org/10.1029/2007JC004712, 2008.

Wakata, Y.: Frequency-Wavenumber Spectra of Equatorial Waves Detected from Satellite Altimeter Data, Journal of Oceanography, 63, 483–490, https://doi.org/10.1007/s10872-007-0043-4, 2007.

Wang, J., Brandt, P., Czeschel, R., Shu, Y., Wang, D., Chen, J., Yang, Y., Huang, K., He, Y., and Tian, Y.: Characteristics, Sources, and Energetics of Yanai Waves in the Equatorial Indian Ocean, Journal of Physical Oceanography, p. e250156, https://doi.org/10.1175/JPO-D-25-0156.1, 2026.

Weisberg, R., Horigan, A., and Colin, C.: Equatorially Trapped Rossby-Gravity Wave Propagation in the Gulf of Guinea, Journal of Marine Research, 37, 1979.

Weisberg, R. H. and Horigan, A. M.: Low-Frequency Variability in the Equatorial Atlantic, Journal of Physical Oceanography, 11, 913–920, https://doi.org/10.1175/1520-0485(1981)011<0913:LFVITE>2.0.CO;2, 1981.

Wheeler, M., Kiladis, G. N., and Webster, P. J.: Large-Scale Dynamical Fields Associated with Convectively Coupled Equatorial Waves, Journal of the Atmospheric Sciences, 57, 613–640, https://doi.org/10.1175/1520-0469(2000)057<0613:LSDFAW>2.0.CO;2, 2000.

Wunsch, C. and Gill, A. E.: Observations of Equatorially Trapped Waves in Pacific Sea Level Variations, Deep Sea Research and Oceanographic Abstracts, 23, 371–390, https://doi.org/10.1016/0011-7471(76)90835-4, 1976.

Yanai, M. and Hayashi, Y.: Large-Scale Equatorial Waves Penetrating from the Upper Troposphere into the. Lower Stratosphere, Journal of the Meteorological Society of Japan. Ser. II, 47, 167–182, https://doi.org/10.2151/jmsj1965.47.3_167, 1969.

Yanai, M. and Maruyama, T.: Stratospheric Wave Disturbances Propagating over the Equatorial Pacific, Journal of the Meteorological Society of Japan. Ser. II, 44, 291–294, https://doi.org/10.2151/jmsj1965.44.5_291, 1966.

Zhang, H., Wang, J., Zhang, Z., Ma, W., Wang, F., and Du, Y.: Observed Deep Intraseasonal Variability in the Western Equatorial Pacific Ocean: Yanai Waves Originated from the Western Boundary, Journal of Physical Oceanography, 55, 2421–2431, https://doi.org/10.1175/JPO-D-25-0031.1, 2025.

Zhu, X.-H., Kaneko, A., Gohda, N., Inaba, H., Kutsuwada, K., and Radenac, M.-H.: Observation of Mixed Rossby-Gravity Waves in the Western Equatorial Pacific, Journal of Oceanography, 54, 133–141, https://doi.org/10.1007/BF02751689, 1998.